Available online at www.sciencedirect.com
SCIENCE DIRECT
Journal of Molecular Structure 789 (2006) 71–80
Journal of MOLECULAR STRUCTURE
www.elsevier.com/locate/molstruc

Structural study of (±) ethyl 3-acyloxy-1-azabicyclo[2.2.2]octane-3-carboxylates by ^{1}H, ^{13}C NMR spectroscopy, X-ray crystallography and DFT calculations

M.S. Arias-Pérez [a,*], A. Cosme [a], E. Gálvez [a], A. Morreale [b], J. Sanz-Aparicio [c], I. Fonseca [c]

[a] Departamento de Química Orgánica, Universidad de Alcalá, 28871 Alcalá de Henares, Madrid, Spain
[b] Unidad de Bioinformática, Centro de Biología Molecular Severo Ochoa, Universidad Autónoma de Madrid, Cantoblanco, 28049 Madrid, Spain
[c] Departamento de Cristalografía, Instituto Rocasolano, C.S.I.C., Serrano 119, 28006 Madrid, Spain

Received 7 November 2005; received in revised form 14 December 2005; accepted 14 December 2005
Available online 14 February 2006

Abstract

^{1}H, ^{13}C NMR spectroscopy and DFT/B3LYP calculations were applied to investigate the conformational preferences of the ethoxycarbonyl and acyloxy groups of some α-acyloxyesters derived from (±) ethyl 3-hydroxy-1-azabicyclo[2.2.2]octane-3-carboxylate. The crystal structure of (±) ethyl 3-diphenylacetoxy-1-azabicyclo[2.2.2]octane-3-carboxylate was determined by X-ray diffraction. To correlate between calculated conformations and the structure in solution, NMR chemical shifts calculations were also performed using the GIAO approach. It has been found that the lowest energetic conformer computed gives the greatest correspondance with experimental solution and solid state data.

Keywords: 3-Acyloxy-1-azabicyclo[2.2.2]octane-3-carboxylates; α-Acyloxyesters; Quinuclidine derivatives; NMR spectroscopy; X-ray crystallography; Conformational study; MM and DFT calculations; Chemical shifts: GIAO/DFT calculations.

1. Introduction

Many natural and synthetic 1-azabicyclo[2.2.2]octane (quinuclidine) derivatives have shown a broad spectrum of biological activities. For example, the quinuclidine system is present in potent agonists and antagonists of muscarinic [1–3] and 5-TH_3 receptors [4,5]. The great number of potential therapeutic applications of these compounds, and the ionotropic receptor ligands in general, has led to an increasing interest to understand the molecular mechanisms operating at the different families of these receptors [4–8].

As a part of a research program devoted to the development of potential ligands for ionotropic receptors, we turned our attention to the synthesis, structural and pharmacological studies of 3,3-disubstituted quinuclidine derivatives [9–11]. We report in this paper a comparative study of several α-acyloxyesters, **2**–**7**, derived from (±) ethyl 3-hydroxy-1-azabicyclo[2.2.2]octane-3-carboxylate (Scheme 1) by means of quantum mechanical calculations and NMR spectroscopy. In these conformationally restricted derivatives fixed conformations of the flexible β-alanine, a ligand of the glycinergic receptor with dual behaviour [12], can be mimicked. Furthermore, these compounds are analogues of the nipecotinic acid that has been shown to be a potent inhibitor of the GABA-uptake process [12]. Owing to the quinuclidine system is a relative rigid moiety, the flexibility of the side chains can play an important role on the ligand–receptor interactions. Theoretical calculations were performed by density functional (DFT) method at the B3LYP/6-311G(d,p) level due to previous studies on (±) alkyl 3-hydroxy-1-azabicyclo[2.2.2]octane-3-carboxylates [11] showed that this approach is relatively more reliable than molecular mechanics and ab initio RHF methods to explain the behaviour of the alkoxycarbonyl groups in these compounds. To correlate between calculated conformations and the structure in solution, NMR chemical shift calculations were carried out using the GIAO approach. In order to gather an accurate description of the conformational preferences of the ethoxycarbonyl and acyloxy groups both in solution and in the solid state, the crystal structure of the (±) ethyl 3-diphenylacetoxy-1-azabicyclo[2.2.2]octane-3-carboxylate, **2**, has also been determined.

* Corresponding author. Tel.: +34 1 8854699; fax: +34 1 8854686.
E-mail address: selma.arias@uah.es (M.S. Arias-Pérez).

0022-2860/$ - see front matter © 2006 Elsevier B.V. All rights reserved.
doi:10.1016/j.molstruc.2005.12.037

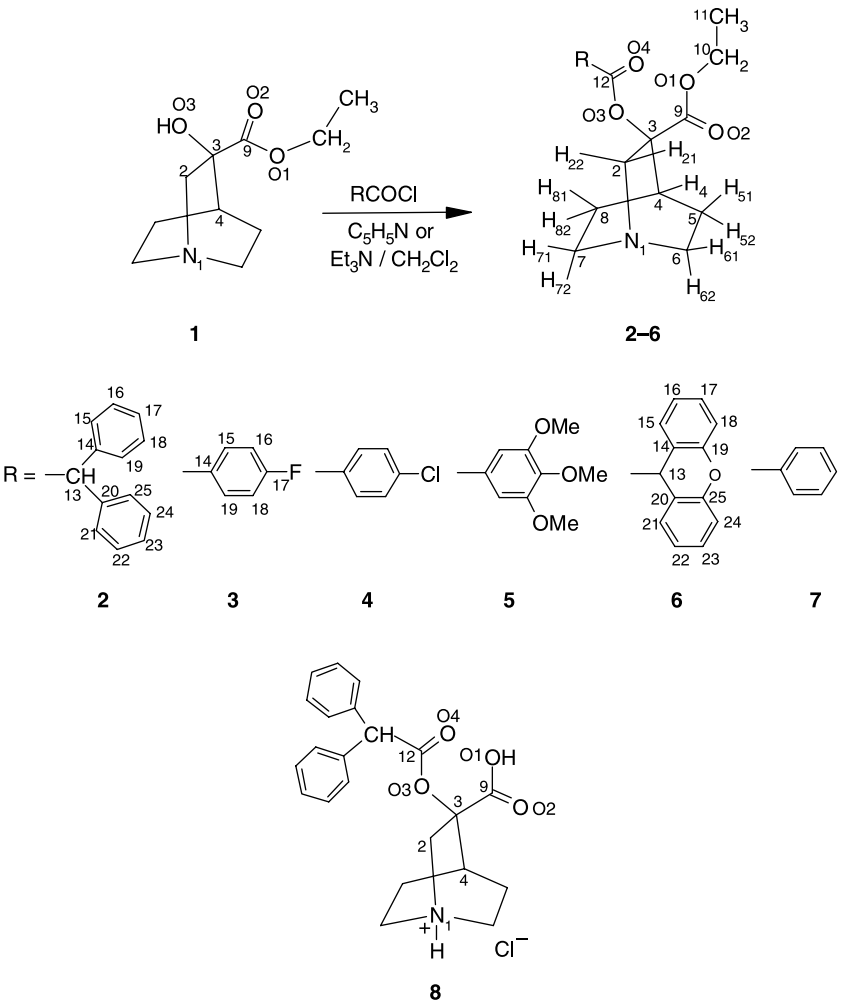

Scheme 1.

2. Experimental

The main crystallographic data and the structure determination conditions for compound **2** are summarised in Table 1 together with the refinement procedures [13–19].

All NMR spectra (^{1}H, ^{13}C, double resonance-decoupling-experiments, DEPT, ^{1}H–^{1}H COSY-45, NOESY and ^{1}H–^{13}C HETCOR) were recorded on a Varian UNITY-300 spectrometer in $CDCl_3$ at 298 K using standard pulse sequences. Lorentz–Gauss transformation (LB = −0.8; GF = 0.6 and GFS = 0.2) was used to improve the resolution of the ^{1}H-NMR spectra [20]. In the case of **6**, the agreement between the observed spectrum and the parameters established from analysis with the LAOCOON III program [21] was verified by simulation of the calculated spectrum.

2.1. Synthesis

The synthesis of the diesters **2–5** was carried out by treatment of the α-hydroxyester **1** with the appropriate acyl chloride (Scheme 1) in dry pyridine at room temperature for 8 days. For **6** the reaction was performed with triethylamine in anhydrous methylene chloride at 20 °C for 4 h, because the xanthene-9-carbonyl chloride readily undergoes decomposition in pyridine. The products were purified by column chromatography (on silica gel for **2–5** and neutral aluminum oxide for **6**) using gradient elution (hexane–ethyl acetate). Compounds **2, 5** and **6** were obtained as solids and recrystallized from hexane (mp (uncorrected), 82–4 °C (**2**), 70–2 °C (**5**) and 107–8 °C (**6**)), while **3** and **4** were isolated as oils. Yield, 44% (**2**), 78% (**3**), 70% (**4**), 23% (**5**) and 37% (**6**).

2.2. Computational details

Theoretical studies were carried for **3** and **7** (Scheme 1). In order to explore lower-energy conformations on the potential energy surface, molecular mechanics calculations were performed first for **7**. The molecule was assembled within Insight II (Accelrys, Inc.) using standard bond lengths and bond angles. Atomic charges were assigned according to Consistent Valence Force Field (CVFF) [22] and molecular mechanics energy minimisations were done with the same force field and with the Adopted Basis Newton–Raphson algorithm [23]. The structures were considered fully optimised

Table 1
Experimental data and structure refinement procedures for **2**

Crystal data	
Formula	$C_{24}H_{27}NO_4$
Crystal size (mm)	0.25×0.31×0.23
Symmetry	Tetragonal, *I* 41 *a*
Unit cell determination	Least-squares fit from 28 reflexions ($0<2\theta<84°$)
Unit cell dimensions	29.143(1), 29.143(1), 10.407(1) Å
	90.0, 90.0, 90.0°
Packing: V(Å^3), Z	8838.5(8), 16
Dc(g cm^{-3}), M, F(000)	1.1828, 393.482, 3360
μ (cm^{-1})	6.11
Experimental data	
Technique	Four circle difractometer: Philips PW 1100; bisecting geometry; graphite oriented monochromator, Cu Kα; $\omega/2\theta$ scans; scanning range for θ: $2<\theta<65°$
Number of reflexions	
Measured	3757
Observed	2526 ($I>3\sigma$(I) criterion)
Range of hkl	0/34, 0/34, 0/12
	No correction applied [13]
Solution and refinement	
Solution	Direct methods and Fourier synthesis
Refinement	Mixed, C10, C26, C11, C27 and H atoms fixed
Variables	265
H atoms	Differential Fourier synthesis and geometric calculations
W-scheme	Empirical as to give no trends in $<w\Delta^2F>$ vs. $<\|Fo\|>$ and $<\sin\theta/\lambda>$ [14]
Final shift/error	0.08
Final R and Rw	0.063, 0.072
Computer programs	VAX 11/750, MULTAN 80 [15], DIRDIF [16], X-RAY76 [17], PARST [18]
Scattering factors	International tables for X-ray crystallography [19]
Anomalous dispersion	International tables for X-ray crystallography [19]

when the energy changes between successive iterations were less than 0.001 kcal/mol. Except otherwise stated the dielectric constant of the medium was set to unity. The conformational performance of the flexible side chains was examined by rotation around the C3–C9, C9–O1, O1–C10, C3–O3, O3–C12 and C12–C14 bonds (Scheme 1). The systematic search method (grid scan), where each specified torsion angle is varied over a grid of equally spaced values, was used; the torsion angles were varied with a step size of 10° from 0 to 360°. In each step these angles were kept fixed while all the other internal coordinates were relaxed. Full energy minimisations with respect to all coordinates were performed for local minima using the same algorithm and parameters as stated above. The conformational energies and energy-minimised geometries of the respective conformations were deduced. Moreover, minimisations were also done with different values for the effective dielectric constant ($\varepsilon=1$, 3, 10 and 80).

Considering that a fluorine atom at the 4-position of the aromatic ring should not practically influence the behaviour of the ethoxycarbonyl and acyloxy groups, similar conformations were assumed for **3**. For the low-energy conformations deduced, density functional calculations were carried out using the B3LYP method and the 6–311G(d,p) basis set. Single point calculations upon optimised geometries were achieved for **3** and **7**. Further geometry optimisations were performed in the case of **3** for a comparison with the conformational properties obtained from the NMR data. The same basis set was used in the calculations of the ^{1}H and ^{13}C chemical shifts for the low-energy conformations by the GIAO/DFT method [24,25]. This approach was chosen because this procedure is considered to provide reliable predictions [26–28] and describes reasonably well the main features of related compounds [11]. The GAUSSIAN 98 package [29] was employed for these calculations.

All the calculations have been performed on a Silicon Graphics O2 workstation and multiprocessor POWER CHALLENGE computer.

3. Results and discussion

3.1. Theoretical calculations

Conformational performance of the α-acyloxyesters **2–7** was examined by the rotation and orientation in the space of the flexible ethoxycarbonyl and acyloxy side chains. For **7** the MM calculations led to six minimum energy conformations within energy differences of less than 16 kcal/mol (Table 2). The arrangement around the C3–O3 and C3–C9 bonds mainly determine the geometry of the side chains. Based on the geometrical similarity of the acyloxy substituent, these forms can be classified into three groups characterised by the torsion angle C12O3C3C4 (ω_1, Scheme 1) and denoted as **A**, **B** and **C** (ω_1 around −169, −81 and 47°, respectively). For each group there are two possible orientations of the ethoxycarbonyl moiety (torsion angle C2C3C9O2) with a similar energy content for a value of the effective dielectric constant $\varepsilon=1$. An increase of the effective dielectric constant from 1 to 80 exerts a small effect on the ratio of the **A** and **B** conformations and the two possible orientations of the ethoxycarbonyl group. However, this change reduces significantly the relative energy content of the **C** forms. In any case, this procedure indicates a strong preference for **A** and **B** conformations, while the **C** forms are strongly destabilised.

Density functional calculations at the B3LYP/6-311G(d,p) level were carried out for **A–C** conformations of **3** and **7**. Single point calculations afforded, as expected, similar relative energies for the selected conformations predicting the same preference for both compounds. Therefore, it seems that the spatial orientations of the side chains should be independent of the nature of the aromatic ring substituents (F in **3** and H in **7**). In light of these findings, further geometry optimisations were performed for **3**. Relative energies and conformational populations computed are collected in Table 3. Some characteristic torsional angles are also tabulated to illustrate the final geometries obtained. A stereoview of these conformations is presented in Fig. 1. This procedure yields much greater energy differences not only between **A** and **B** forms, but also between the two possible orientations of the ethoxycarbonyl moiety. However, their interconversion

Table 2
Relative energies, populations and selected torsion angles for the significant conformations of **7** computed using the MM method

	A-1	A-2	B-1	B-2	C-1	C-2
C12O3C3C4	−168	−169	−84	−79	46	48
C2C3C9O2	22	−163	112	−63	−2	146
C10O1C9C2	−24	17	22	−19	−5	2
C3O3C12O4	−23	−18	44	21	74	73
O4C12C14C15	−1	−1	0	1	−4	−2
C9O1C10C11	−172	176	172	−176	−179	180
E_r (kcal/mol)/N_i						
$\varepsilon=1$	0.00/0.33	0.07/0.30	0.37/0.18	0.33/0.19	15.22/–	15.21/–
$\varepsilon=3.0$	0.00/0.34	0.34/0.19	0.01/0.34	0.56/0.13	9.26/–	9.92/–
$\varepsilon=10.0$	0.00/0.39	0.54/0.16	0.08/0.34	0.73/0.11	7.49/–	8.42/–
$\varepsilon=80.0$	0.00/0.41	0.62/0.15	0.14/0.33	0.79/0.11	6.86/–	7.90/–

requires a low additional cost (lesser than 3.2 kcal/mol). According to this method, the **A** forms should dominate the conformational equilibrium to the extent of 94% at room temperature, followed by a small contribution (6%) of the **B** conformations. The **C** forms are also the most unfavourable and their participation may be negligible.

The B3LYP method shows that the relative orientation of the alkoxy C9–O1 and O3–C12 bonds is practically fixed in a planar *Z* conformation (torsion angles C10O1C9O2 and C3O3C12O4 around 0°). These features are in concordance with the behaviour reported for alkoxycarbonyl groups [10,11,30]. As expected, the aryl group of the acyloxy moiety can adopt two symmetric and isoenergetic conformations in which the carbonyl and the aryl groups are coplanar (torsion angle O4C12C14C15 about 0°). Moreover, the energy content of the three staggered dispositions around the O1–C10 bond of the ethoxycarbonyl substituent is very close with a slight predominance of the *anti* orientation of the methyl group with respect to C-9.

Concerning the bonds connecting the side chains with the bicyclic system, this procedure showed that the C3–O3 fragment should display practically a staggered conformation where the carbonyl carbon C-12 is in an *anti* arrangement with respect to the bicyclic carbon C-4 (**A** forms, torsion angle C12O3C3C4 = −175°, 94%). The C3–C9 fragment adopts almost eclipsed conformations with different degrees of distortion from the ideal geometry, similar to those reported for the alkoxycarbonyl group of (±) alkyl 3-hydroxy-1-azabicyclo[2.2.2]octane-3-carboxylates [11] using the same method. The preferred spatial arrangement (86%) for the ethoxycarbonyl group of the α-acyloxyester **3** was found to be a slightly distorted C=O/C2 eclipsed conformation (**A-1**, torsion angle C2C3C9O2 = 25°). The two alternative forms in which the carbonyl group is almost eclipsed with the dicoordinate oxygen atom of the acyloxy group (O-3) and the bridgehead carbon C-4 (**A-2** and **B-1**, respectively) should amount to about 14% of the equilibrium mixture, with practically the same participation. For the α-hydroxyesters the B3LYP calculations predicted that the C=O/O3 eclipsed conformation should be additionally stabilised by a weak intramolecular hydrogen bond between the carbonyl oxygen atom and the OH group, leading to a clear predominance of this

Table 3
Relative energies, populations and selected torsion angles for the significant conformations of **3** computed using B3LYP level of theory and 6–311G(d,p) basis set. Comparative analysis with crystal structures of **1**, **2** and **8**

	A-1[a]	A-2	B-1	B-2	C-1	C-2	X-ray		
							2	8	1
C12O3C3C4	−175	−175	−73	−74	86	97	−178	−179	
C12O3C3C2	69	69	172	171	−39	−26	66	65	
C2C3C9O2	25	−161	99	−66	3	133	21	19	−179
C4C3C9O2	−94	77	−21	172	−116	12	−99	−100	63
O3C3C9O2	151	−37	−146	47	126	−102	145	144	−58
C2C3C9O1	−159	22	−76	111	−178	−48	−165	−165	2
C10O1C9O2	−5	3	5	−4	0	2	−11(6)[b]		3
C3O3C12O4	−1	2	0	1	−6	−5	7	12	
O4C12C14–C15	−3	−3	2	1	1	1			
C9O1C10–C11	180	179	180	−179	177	180	−105		174
E_r (kcal/mol)	0.0000	1.4195	1.5891	3.1593	7.0410	8.1025			
N_i	0.859	0.078	0.059	0.004	–	–			

All values correspond to fully optimised geometries.

[a] Relative energies for the three staggered conformations around the O1–C10 bond: 0.0000, 0.1193 and 0.3706 kcal/mol (torsion angle C9O1C10C11 = 180, −85 and 88°, respectively).

[b] Two values were determined for this torsion angle because the two terminal atoms of the ethoxycarbonyl chain are disordered between two sides.

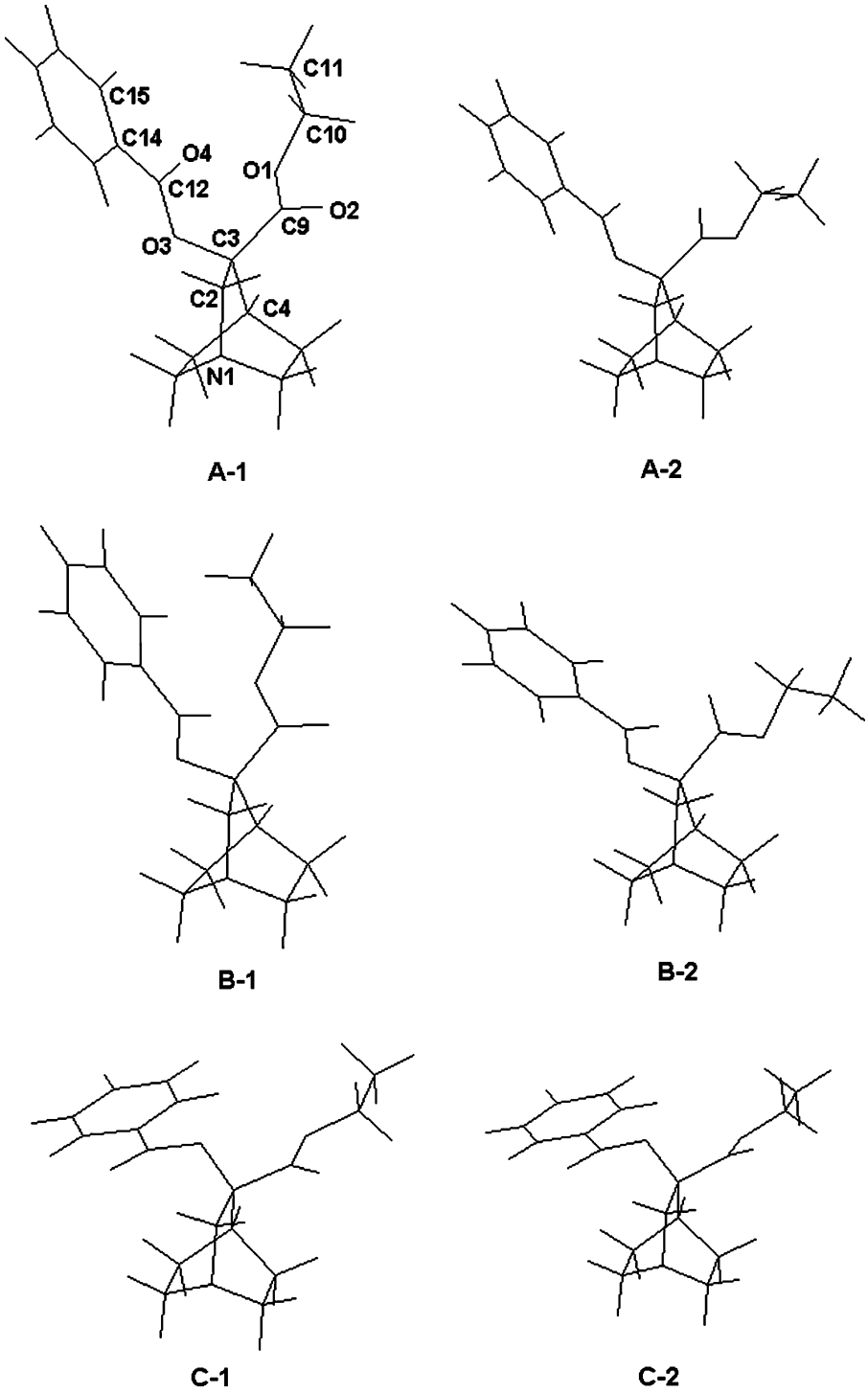

Fig. 1. Stereoview of the preferred conformations of the ethoxycarbonyl and acyloxy groups in **3**

orientation (71%) [11]. Therefore, it seems that the replacement of the hydroxy group with an acyloxy moiety exerts a significant effect on the conformational preferences of the alkoxycarbony side chain of these quinuclidine derivatives. This behaviour may be attributed to a combination of steric and charge factors [11,30]. As a result, the carbonyl groups of both the ethoxycarbonyl and acyloxy side chains in **3** are mainly almost eclipsed with the bicyclic carbons C-2 and C-3, respectively (**A-1** conformation); this form places the carbonyl groups in an almost perpendicular arrangement (dihedral angle between the planes of the carbonyl groups about 105°), probably due to the destabilising through-space interactions of the lone pairs of oxygen atoms.

3.2. Comparison of the X-ray and calculated structures

To compare the theoretical results with experimental data, the X-ray structure of **2** was determined. The PLUTO view

of the molecule, together with the atomic numbering is shown in Fig. 2. CCDC 288076 contains the supplementary crystallographic data for this paper. These data can be obtained free of charge via www.ccdc.cam.ac.uk/conts/retrieving.html (or from the Cambridge Crystallographic Data Centre, 12, Union Road, Cambridge CB2 1EZ, UK; fax: +44 1223 336033).

Each six-membered ring of the quinuclidine moiety adopts practically a boat conformation and the biggest distortion correspond to the N1, C2, C3, C4, C8, C7 ring. The torsion angle values, C6–N1···C4–C5 = 1.7°, C2–N1···C4–C3 = 2.9° and C7–N1···C4–C8 = 2.1°, are similar to those found in the parent hydroxyester **1** [10], but smaller than those reported for other disubstituted quinuclidines [9,31,32], and even for monosubstituted derivatives [33,34]. This fact displays the small influence of the substituents on the conformation of the bicyclic system. All bond distances and valence angles correspond to the expected values [9,10,31,32].

Both phenyl groups form an angle of 80.3(1)° and are perpendicular to the plane of the carbonyloxy group (O3, O4, C12, C13), with angles of 92.6(1) and 93.4(1)°, respectively. The two terminal atoms of the ethoxycarbonyl chain are disordered between two sides (C10–C26, C11–C27) with occupancy factors of 0.5. However, the C10–C27 and C11–C26 lengths are very long and very short (1.628(8) and 1.211(13) Å), respectively. This might be due to no completely resolved disorder as indicated by their high thermal factors, which were fixed after isotropic refinement.

The molecules are held together in the crystal by means of a hydrogen bonding network constituted by the nitrogen atom that accepts an hydrogen atom of a water molecule, which, on the other hand, donates the other hydrogen atom to another crystallisation water. The geometry of the hydrogen bonds is as follows: O28–H281 = 0.962(4), O28—N1 = 2.805(5), H281···N1 = 1.902(3) Å, O28–H281···N1 = 155.3(4)° (*x*,*y*,*z*); O28–H282 = 1.079(4), O28···O28 = 2.678(5), H282···O28 = 1.642(4) Å, O28-H282···O28 = 159.2(3)°; (*y*, $-x+1/2$, $z+1/4$).

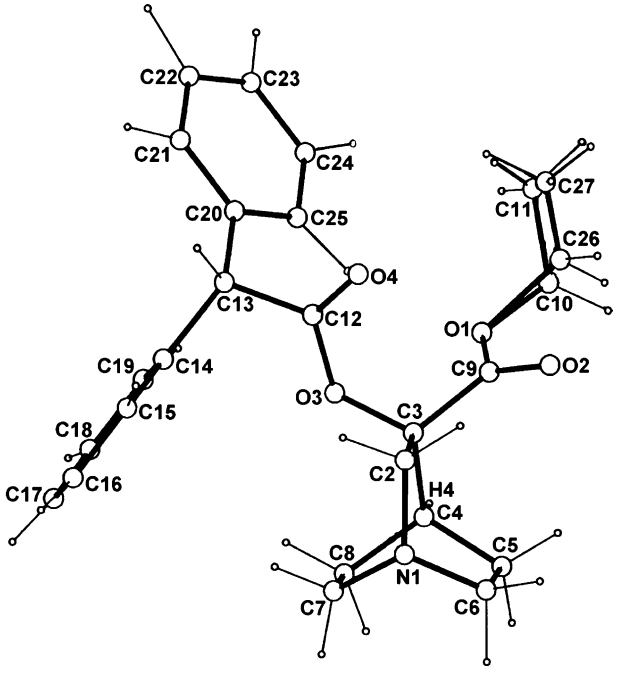

Fig. 2. PLUTO view of **2** showing the atomic numbering.

The crystal structure of **2** confirms the same behaviour of the α-acyloxyesters **2**–**7** in the gas phase (theoretical calculations) and the solid state. The good agreement between experimental torsion angles determined for **2**, and those calculated for the conformation **A-1** of **3** (Table 3) supports the correctness of the calculations. The different disposition of the methyl group of the ethoxycarbonyl side chain (torsion angle C9O1C10C11 = −105° in the solid state and 180° for the more favourable orientation computed) may be ascribed to the packing in the crystal structure. Owing to theoretical calculations account for very low energy differences between the three staggered dispositions around the O1-C10 bond, their interconversion can take place easily. A similar preference was found for the carboxylic and diphenylacetoxy groups of the (±) 3-diphenylacetoxy-1-azabicyclo[2.2.2]octane-3-carboxylic acid hydrochloride, **8**, (Scheme 1, Table 3) in the solid state [9].

On the other hand, a different orientation of the ethoxycarbonyl moiety was observed for the α-hydroxyester **1** in the solid state [10]. In this case, the carbonyl group adopts an almost ideal staggered (bisecting) arrangement with respect to the bicyclic carbon C-4 and the oxygen atom of the hydroxy group (O-3) while the dicoordinate oxygen atom (O-1) is practically eclipsed with the bicyclic carbon C-2 (torsion angles: C4C3C9O2 = 63°, O3C3C9O2 = −58° and C2C3C9O1 = 2°, Table 3). It was suggested [11] that the change in the spatial orientation of the ethoxycarbonyl group could be facilitated by the strong intermolecular hydrogen bonds between the OH group and the bicyclic N atom in the crystal structure. The staggered form adopted in the solid state would be more favourable for their formation due to the OH is sterically more accessible. These results confirm the flexibility of the ethoxycarbonyl group in these quinuclidine derivatives and the strong dependence on intra and intermolecular interactions as was previously suggested.

Pharmacologically interesting is the spatial arrangement of the structural fragment C9C3C4C8 in **2**, close to that reported for **1** [10] and **8** [9], which shows a reasonably good concordance with one of the bioactive conformations proposed for the GABA molecule [35]. Moreover, the conformation of this fragment is similar to the related Cα–Cβ and Cβ–Cγ bonds in the selective $GABA_B$ receptor agonist baclofen in solid state (baclofen·HCl) [36,37]. On the other hand, **1**, **2** and **8** exhibit a value of the intramolecular distance N1···O3, (3.44 Å in **2**) similar to that reported for the 3-quinuclidinol (∼3.5 Å) [3].

3.3. NMR study

The derivatives **2**–**6** were studied in depth by ^{1}H and ^{13}C NMR in $CDCl_3$. The assignment of the bicyclic proton and carbon resonances was achieved by the combined use of 2D-NMR techniques, homonuclear spin decoupling experiments

and our previous studies on related quinuclidine derivatives [9–11,32].

The ^{13}C NMR chemical shifts are tabulated, with the signal assignments, in Table 4. Substituent steric and electronic effects on the ^{13}C chemical shifts [38,39] were taken into consideration. The distinction between the C-5 and C-8 resonances can be readily inferred on the basis of the different upfield-shifting γ-gauche effects exerted by the ethoxycarbonyl and acyloxy groups [38,39]. Taking into account that a greater value has been reported for the γ-gauche effect exerted by an acyloxy group (ca. 5 vs. 3 ppm) on the bicyclic carbons of the quinuclidine system [9,10], the signal at highest-field (20 ppm) must correspond to C-8 (Scheme 1). Moreover, the chemical shift difference between C-5 and C-8 carbons—ca. 2.3 ppm— is similar to that found for related α-hydroxyesters (**1**, Table 4) [10].

At 300 MHz the ^{1}H NMR spectra of **2–6** are very similar. The interpretation of the ^{1}H–^{1}H COSY spectra was based on the unambiguous assignment of the signals for H-4 and C-2 protons, owing to their shape and chemical shifts. These signals are well differentiated, while the other bicyclic proton resonances exhibit higher complexity and appear partially overlapped as ill-resolved multiplets, except for **6**. That only could perform the identification and assignment of all bicyclic protons for **6**.

The differentiation between the signals of C-5 and C-8 protons could be made from the heteronuclear ^{1}H–^{13}C correlated spectra, once the resonances of the respective carbons were known. Thus, in the case of **6**, the observation of the following correlations $\delta = 20.1/1.59$ and 1.24 ppm and $\delta =$ 22.5/1.48 and 1.42 ppm allows the assignment of the multiplets at 1.59 and 1.24 ppm to the C-8 protons, while the C-5 protons resonate at 1.48 and 1.42 ppm. The C-6 and C-7 protons were assigned on the basis of their correlations with the C-5 and C-8 protons. From these statements, the assignment of the diastereotopic protons of each methylene group was based on the analysis of the COSY cross-peaks due to W long-range couplings (^{4}J) and the coupling modifications observed in irradiation experiments. Moreover, the 2D NOESY spectrum corroborated the assignment of H-21 and H-22. The NOESY cross-peaks observed between the signals of aromatic protons and those centred at 2.47 and 1.59 ppm point out the expected proximity of H-22 and H-81 with the aromatic protons. Finally, the analysis of the ^{1}H–^{13}C correlated spectrum allowed the distinction between the chemical shifts of C-6 and C-7, once the resonances of the respective protons were established.

The same trend was assumed for **2–6** bearing in mind the similarity of the ^{1}H NMR spectra. The proton chemical shifts are shown in Table 5. For **6** the multiplets due to C-5, C-6, C-7 and C-8 protons were considered as parts of the respective spin systems and analysed with the LAOCOON III program [21]. The observed ^{1}H–^{1}H coupling constants for the quinuclidine moiety are very similar to those described for related compounds [9–11,32]. The values deduced for **6** are given in Table 5.

The comparison of the proton chemical shifts of derivatives **2–6** with those reported for the parent α-hydroxyester **1** (Table 5) [10] indicates that H-71 and H-81 are shielding in **2** and **6** around 0.4 ppm. This effect also supports the correctness of the previous considerations about the proton assignments, and accounts for a spatial orientation in which these protons lie near to the shielding region of the aromatic rings [20]. The nature of the acyloxy group in **3–5** (Scheme 1) does not allow this proximity. The greater value of $\Delta\delta$ H21–H22 in derivatives **2–6** (ca. 1.2 ppm) could be attributed to the change from the free OH to the acyloxy group. However, this change exerts a small influence on the chemical shifts of the bicyclic carbons

Table 4
^{13}C chemical shifts for **1** and the α-acyloxyesters **2–6** in $CDCl_3$

Chemical shifts δ (ppm)[a]	**1**	**2**[b]	**3**[c]	**4**	**5**[d]	**6**[b]
C-8	20.3	20.0	20.5	20.4	20.7	20.1
C-5	22.9	22.6	22.8	22.7	22.8	22.5
C-4	31.5	28.8	29.1	29.0	29.2	28.7
C-6	45.9	45.5	45.7	45.5	45.7	45.6
C-7	46.5	46.4	46.6	46.5	46.6	46.5
C-2	58.3	57.4	57.8	57.6	57.8	57.4
C-3	74.0	80.3	80.5	80.5	80.4	80.5
C-10	61.8	61.3	61.4	61.3	61.3	61.3
C-11	14.2	13.7	13.9	13.8	13.9	13.8
C-9		171.1[e]	171.1	170.9	171.1	170.7[e]
C-12		171.0[e]	164.6	164.6	165.1	170.3[e]
C-14(C-20)		137.7; 138.1	125.9	128.0	124.6	117.8; 118.0
C-15(C-21)		128.3[e]	132.1	130.8	107.4	129.2; 129.3[e]
C-16(C-22)		128.5[e]	115.5	128.6	153.0	123.2; 123.3
C-17(C-23)		127.1; 127.3	165.8	143.1	143.1	128.7; 128.8[e]
C-18(C-24)		128.3	115.5	128.6	153.0	116.9; 117.0
C-19(C-25)		128.5	132.1	130.8	107.4	151.2; 151.3

[a] Error ±0.1 ppm.
[b] C-13: 56.7 (**2**) and 45.4 ppm (**6**).
[c] ^{1}JC17-F = 254.6 Hz; $|^{2}J$C16(18)-F$|$ = 22.2 Hz; ^{3}JC15(19)-F = 9.5 Hz; $|^{4}J$C14-F$|$ = 2.9 Hz.
[d] Ar**OCH$_3$**: 60.6 (1) and 56.2 ppm (2).
[e] Tentative assignment.

Table 5
^{1}H chemical shifts for **1** and the α-acyloxyesters **2-6** in $CDCl_3$

Chemical shifts δ (ppm)[a,b]	**1** [10]	**2**	**3**	**4**	**5**[c]	**6**
H-21 (dd)[d]	3.51	3.93	4.08 (d)	4.08 (d)	4.08 (d)	3.78
H-22 (dd)[d]	2.71	2.65	2.88 (d)	2.88 (d)	2.88 (d)	2.47
H-61	2.77–2.67	2.88	3.02–2.76	3.02–2.76	3.01–2.76	2.80[e]
H-72	2.82	2.79–2.69	3.02–2.76	3.02–2.76	3.01–2.76	2.70[e]
H-62	2.77–2.67	2.79–2.69	3.02–2.76	3.02–2.76	3.01–2.76	2.65[e]
H-71	2.88	2.48	3.02–2.76	3.02–2.76	3.01–2.76	2.34[e]
H-4	1.90	2.14	2.32	2.33	2.34	2.00
H-81	2.07	1.73	2.14	2.15	2.14	1.59[e]
H-51	1.57	1.62–1.46	1.72–1.49	1.67–1.49	1.69–1.50	1.48[e]
H-52	1.50	1.62–1.46	1.72–1.49	1.67–1.49	1.69–1.50	1.42[e]
H-82	1.32	1.36–1.31	1.72–1.49	1.67–1.49	1.69–1.50	1.24[e]
H-10	4.22 (q)	4.13 (q)[f]	4.25[g]	4.24[g]	4.24 (q)[f]	4.04[g]
		–	4.20[g]	4.20[g]	–	3.98[g]
H-11	1.25 (t)	1.12 (t)[f]	1.21[g]	1.21[g]	1.24 (t)[f]	1.03[g]
H-13(s)		5.07				5.00

[a] Abbreviations: d, doublet; dd, doublet of doublets; m, multiplet; q, quartet; s, singlet; t, triplet. Error, $\delta \pm 0.01$ ppm; $J \pm 0.1$ Hz.

[b] Aromatic protons δ: **2**, 7.36–7.26 (m, 10H); **3**, 8.07, 7.14 (AA'MM'X system due to the fluorine atom, ^3JH15–H16 = ^3JH18–H19 = 8.9, ^3JH16(18)–F = 8.6, $|^4J$H15(19)–$F|$ = 5.4 Hz); **4**, 7.99 (d, 2H, J = 8.4 Hz), 7.44 (d, 2H, J = 8.4 Hz); **5**, 7.31(s, 2H); **6**, 7.31 (dd, 2H, J = 8.0 and 7.3 Hz), 7.29 (d, 2H, J = 7.4 Hz), 7.15 (dd, 2H, J = 8.0 and 1.3 Hz), 7.09 (m, 2H, J = 7.4, 7.3 and 1.3 Hz).

[c] OCH_3, δ = 3.92 (s, 9H).

[d] ^2JH21–H22 = −15.0 Hz (**2–6**); $|^4J$H21–H72| = 2.3 and $|^4J$H22–H62| = 2.1 Hz for **2**.

[e] Values deduced from the analysis of the respective spin subsystems with the LAOCOON III program: ABCDXY (**H-61**, **H-62**, H-22, H-71, H-51 and H-52); AMNPXZ (H-21, H-61, **H-72**, **H-71**, H-81 and H-82); ADMPQX (H-72, H-71, H-4, **H-81**, H-51 and **H-82**); ABPXYZ (H-61, H-62, H-4, H-81, **H-51** and **H-52**). ^2JH51–H52 = −13.43, ^2JH61–H62 = −13.18, ^2JH71–H72 = −13.38, ^2JH81–H82 = −13.32, ^3JH4–H51 = 2.68, ^3JH4–H52 = 3.42, ^3JH4–H81 = 3.26, ^3JH4–H82 = 2.46, ^3JH51–H61 = 10.42, ^3JH51–H62 = 5.62, ^3JH52–H61 = 5.86, ^3JH52–H62 = 10.00, ^3JH71–H81 = 10.27, ^3JH71–H82 = 5.98, ^3JH72–H81 = 4.22, ^3JH72–H82 = 10.71, $|^4J$H21–H72| = 2.44, $|^4J$H22–H62| = 1.95, $|^4J$H51–H81| = 3.08, $|^4J$H61–H71| = 2.67 Hz; error ± 0.05 Hz.

[f] ^3JH10–H11 = 7.1 Hz.

[g] These protons appear as an ABX_3 system: ^2JH101–H102 = −10.9 (**3**), −10.7 (**4**) and −10.8 Hz (**6**); ^3JH10–H11 = 7.1 Hz.

(except on C-3) (Table 4). Also coplanarity between the carbonyl and aryl groups of the acyloxy moiety in **3–5** can be assumed owing to the chemical shifts of the carbonyl carbon [38,39].

To obtain additional information, theoretical ^{1}H and ^{13}C chemical shifts were also calculated for **A–C** conformations of **3** by the GIAO/DFT method, and compared to the experimental data. In general, the experimental values are more consistent with those computed for **A** forms (Table 6), in agreement with the previous hypothesis.

The most relevant information about the conformational preferences of the substituents is derived from the proton chemical shifts. Similar values were obtained for **A** forms, while remarkable variations among these conformations and the other orientations were predicted for the bicyclic protons which are near to the esters moieties (Table 6). The different orientation of the carbonyl groups and the balance of their anisotropic effects [38,39] seem to be the main cause of these changes. Thus, in **A** and **C-1** forms, H-21 lies near the plane of C9=O2 group in concordance with the values of the torsion angle C2C3C9O2 (Table 6, Fig. 1), and is more deshielding (ca. 1.2 ppm) than in the other orientations. The C12=O4 group exerts a similar effect on H-22 and H-71 in **C** forms. The downfield shift is particularly large for H-22 in the **C-2** conformation (2.3 ppm with respect to **A** forms). As a result, H-22 resonates at higher field than H-21 in **A** forms. Reverse order was predicted for **B** and **C** orientations in contradiction with experimental shifts. Moreover, the $\Delta\delta$H21–H22 for compounds **2–6** was found to be practically constant and independent of the nature of the acyloxy moiety, with a value about 1.2 ppm (Table 5), similar to that calculated for **A** conformations. These findings and the reasonably good agreement between the observed and calculated (average) values also support a marked predominance of **A** forms in solution. A limiting value of around 10% was deduced for the participation of the **B** orientations in the conformational equilibrium from the estimated proton shifts. In any case, the contribution of **C** forms can be reasonably disregarded. However, the relative stability of the **A-1** and **A-2** conformations could not be established from these data.

Concerning ^{13}C chemical shifts, significant deviations between the calculated and experimental values were obtained (Table 6, standard deviations (SD) = 6.7 (**A-1** and **B-2**), 6.9 (**A-2**), 6.6 (**B-1**), 7.8 (**C-1**) and 7.6 (**C-2**)), probably due to solvent effects and/or the inability of the calculation method to reproduce accurately the ^{13}C chemical shifts for these derivatives [27]. However, the predicted shifts follow the same trend and account for a small dependence of these parameters on the conformational changes of the side chains. The most significant difference among conformations appears for the chemical shifts of the quaternary carbon C-3 that is strongly deshielding in **C** forms (ca. 8 ppm), showing the largest deviation from the experimental value. On the other hand, the best correlation between experimental and calculated values for $\Delta\delta$C5–C8 corresponds to **A** conformations.

Table 6
Comparative analysis between experimental chemical shifts and theoretical values calculated over B3LYP/6-31G(d,p) optimised geometries for **3**.

Chemical shifts δ (ppm)[a]	**A-1**	**A-2**	**B-1**	**B-2**	**C-1**	**C-2**	**Avg**[b]	**Exp**
H-21	4.24	4.22	2.96	2.93	3.91	3.00	4.16	4.08
H-22	2.81	2.91	3.32	3.45.	4.23	5.15	2.85	2.88
H-61	2.95	2.90	2.79	2.75	2.73	2.56	2.94	2.76–3.02
H-71	2.82	2.79	2.84	2.88	3.62	3.79	2.82	2.76–3.02
H-4	2.06	2.13	2.94	2.92	2.35	2.36	2.12	2.32
H-81	2.17	2.21	1.56	1.56	2.15	1.72	2.13	2.14
H-51	1.57	1.53	2.80	2.31	1.26	1.99	1.64	1.49–1.72
C-8	25.8	26.3	27.9	28.4	27.1	26.8	26.0	20.5
C-5	28.7	28.7	27.1	27.6	32.3	29.7	28.6	22.8
C-4	36.9	37.9	33.5	32.6	40.0	37.1	36.8	29.1
C-6	50.9	51.1	52.7	52.5	50.8	53.0	51.0	45.7
C-7	51.8	52.2	51.3	51.6	51.4	50.3	51.8	46.7
C-2	64.9	64.6	65.8	65.7	54.2	56.5	64.9	57.8
C-3	88.0	87.7	88.0	87.9	95.2	97.0	88.0	80.5

[a] The remaining chemical shifts have very close values in all conformations. Average values, δ ^{1}H: H-72, 2.76; H-62, 2.63; H-52, 1.24; H-82, 1.23; H-10, 4.11 and 4.00; H-11 (estimated as the medium value of the calculated chemical shifts for each proton of the methyl group), 1.12; H-15, 8.28; H-16, 7.12; H-18, 7.19; H-19, 8. 41 ppm; δ ^{13}C: C-10, 66.5; C-11, 15.7; C-14, 132.6; C-15, 140.2; C-16, 120.8; C-17, 176.2; C-18, 120.2; C-19, 138.0; C-9, 179.7; C-12, 170.2 ppm.
[b] Population-weighted values.

Moreover, excellent linear relationship has been observed between experimental ^{13}C chemical shifts (δ_{exp}) and the weighted average values calculated for the three most stable conformations (δ_{calc}). Linear regression analysis gives the following Eq. (1):

$$\delta_{calc} = 1.018\delta_{exp} + 4.624,\ R^2 = 0.999 \quad (1)$$

A comparable relationship (Eq. (2)) was obtained by doing linear regression analysis for **3** and the related methyl 3-hydroxy-1-azabicyclo[2.2.2]octane-3-carboxylate [11].

$$\delta_{calc} = 1.026\delta_{exp} + 3.177,\ R^2 = 0.999 \quad (2)$$

Again, these findings suggest that the lowest energetic conformations **A-1** and **A-2** are the predominant in solution.

4. Conclusions

In summary, the density functional (DFT/B3LYP) calculations satisfactorily reproduce the conformational preferences of the acyloxy and ethoxycarbonyl groups in (±) ethyl 3-acyloxy-1-azabicyclo[2.2.2]octane-3-carboxylates, both in $CDCl_3$ solution and in the solid state. The acyloxy group always prefers a staggered orientation where the carbonyl carbon and the bicycic carbon C-4 are *antiperiplanar*. The ethoxycarbonyl moiety can adopt three almost eclipsed forms by rotation around the C–C(=O) bond. In any case, the carbonyl groups of both side chains display an almost perpendicular arrangement. The lowest energetic conformation computed in gas phase was found to be a slightly distorted C=O/C2 eclipsed form, which equates very well with the crystal X-ray structure. The obtained results indicate that conformational effects on both carbon and proton chemical shifts may be useful for the establishment of the conformational preferences of the substituents in solution. Particularly, chemical shifts of bicyclic protons seem to be highly sensitive to the geometry of the side chains. From these data a limiting value of around 10% for the C=O/C4 eclipsed conformation and a clear predominance of the alternative forms can be proposed in $CDCl_3$ solution.

Acknowledgements

We Thank Dr Avelino Martín for several helpful comments. This work was supported by the Spanish Comisión Interministerial de Ciencia y Tecnología (Project BQU 2002-02576) and the University of Alcalá.

References

[1] J. Saunders, M. Cassidy, S.B. Freedman, E.A. Harley, L.L. Iversen, C. Kneen, A.M. McLeod, K.J. Merchant, R.J. Snow, R. Baker, J. Med. Chem. 33 (1990) 1128.
[2] V.I. Cohen, R.E. Gibson, L.H. Fan, R. De la Cruz, M.S. Gitler, E. Hariman, R.C. Reba, J. Med. Chem. 34 (1991) 2989.
[3] F.I. Carrol, P. Abraham, K. Parham, R.C. Griffith, A. Ahmad, M.M. Richard, F.N. Padilla, J.M. Witkin, P.K. Chiang, J. Med. Chem. 30 (1987) 805.
[4] A. Morreale, I. Iriepa, E. Gálvez, Curr. Med. Chem. 9 (2002) 99.
[5] F.D. King, J.B. Jones, G.J. Sanger, 5-Hydroxytryptamine-3-receptor Antagonists, CRC Press, Boca Raton, FL, 1994.
[6] M.H. Aprison, E. Gálvez, K.B. Lipkowitz, J. Neurosci. Res. 43 (1996) 127.
[7] R.A. Glennon, M. Dukat, Pharm. Acta Helv. 74 (2000) 103.
[8] P. Krogsgaard-Larsen, B. Frlund, U. Kristiansen, K. Frydenvang, B. Ebert, Eur. J. Pharm. Sci. 2 (1997) 355.
[9] M.S. Arias-Pérez, A. Cosme, E. Gálvez, M.J. Santos, M. Martinez-Ripoll, E. Matesanz, J. Mol. Struct. 565–566 (2001) 353.
[10] M.S. Arias-Pérez, A. Cosme, E. Gálvez, J. Sanz-Aparicio, I. Fonseca, J. Bellanato, J. Mol. Struct. 644 (2003) 171.
[11] M.S. Arias-Pérez, A. Cosme, E. Gálvez, A. Morreale, J. Mol. Struct. 655 (2003) 125.
[12] V. Schmieden, H. Betz, Mol. Pharmacol. 48 (1995) 919.
[13] N. Walker, P. Stuart, Acta Crystallogr. A39 (1983) 158.
[14] M. Martinez-Ripoll, F.H. Cano, PESOS: A Computer Program for the Automatic Treatment of Weighting Schemes, Institute Rocasolano, CSIC, Madrid, Spain, 1975.
[15] P. Main, S.J. Fiske, S.E. Hull, L. Lessinger, G. Germain, J.-P. Declercq, M.H. Woolfson, MULTAN 80: A System of Computer Programs for Automatic Solution of Crystal Structures from X-ray Diffraction Data, University of York, England, 1980.

[16] P.T. Beurkens, W.P. Bosman, H.M. Doesburg, R.O. Gould, T.E.M. Van der Hark, P.A.J. Prick, J.H. Noordik, G. Breurken, V. Parthasarathi, DIRDIF, Crystallography Laboratory, Tournooiveld, 6525ED, Nijmegen, The Netherlands, 1982.
[17] J.M. Stewart, P.A. Manchin, C.L. Dickinson, H.L. Ammon, H. Heck, H. Flack, The X-Ray 76 System, Technical Report TR-446, Computer Science Center, University of Maryland, College Park, MD, 1976.
[18] M. Nardelli, Comput. Chem. 7 (1983) 95.
[19] International Tables for X-Ray Crystallography, vol. 4, Kynoch Press, Birmingham, England, 1974.
[20] H. Günther, NMR Spectroscopy, Wiley, Chichester, 1995.
[21] S. Castellano, A.A. Bothner-By, J. Chem. Phys. 41 (1963) 3863.
[22] P. Dauber-Osguthorpe, V.A. Roberts, D.J. Osguthorpe, J. Wolff, M. Genest, A.T. Hagler, Proteins 4 (1998) 31.
[23] B.R. Brooks, R.E. Bruccoleri, B.D. Olafson, D.J. States, S. Swaminathan, M. Karplus, J. Comput. Chem. 4 (1983) 187.
[24] K. Wolinski, J.F. Hilton, P. Pulay, J. Am. Chem. Soc. 112 (1990) 8251.
[25] J. Gauss, Chem. Phys. Lett. 191 (1992) 614.
[26] T. Kupka, G. Pasterna, M. Jaworska, A. Karali, P. Dais, Magn. Reson. Chem. 38 (2000) 149.
[27] E. Virtanen, M. Nissinen, R. Suontamo, J. Tamminen, E. Kolehmainen, J. Mol. Struct. 649 (2003) 207.
[28] S. Saen-oon, S. Hannongbua, P. Wolschann, J. Chem. Inf. Comput. Sci. 43 (2003) 1412.
[29] M.J. Frisch, G.W. Trucks, H.B. Schlegel, G.E. Scuseria, M.A. Robb, J.R. Cheeseman, V.G. Zakrzewski, J.A. Montgomery, Jr., R.E. Stratmann, J. C.Burant, S. Dapprich, J.M. Millam, A.D. Daniels, K.N. Kudin, M.C. Strain, O. Farkas, J. Tomasi, V. Barone, M. Cossi, R. Cammi, B. Mennucci, C. Pomelli, C. Adamo, S. Clifford, J. Ochterski, G.A. Petersson, P.Y. Ayala, Q. Cui, K. Morokuma, D.K. Malick, A.D. Rabuck, K. Raghavachari, J.B. Foresman, J. Cioslowski, J.V. Ortiz, A.G. Baboul, B.B. Stefanov, G. Liu, A. Liashenko, P. Piskorz, I. Komaromi, R. Gomperts, R.L. Martin, D.J. Fox, T. Keith, M.A. Al-Laham, C.Y. Peng, A. Nanayakkara, C. Gonzalez, M. Challacombe, P.M.W. Gill, B.G. Johnson, W. Chen, M.W. Wong, J.L. Andres, M. Head-Gordon, E.S. Replogle, J.A. Pople, GAUSSIAN 98 (Revision A9), Gaussian, Pittsburgh PA, 1998.
[30] E.L. Eliel, S.H. Wilen, N. Mander, Stereochemistry of Organic Compounds, Wiley, New York, 1994.
[31] A. Suszko-Purzycka, T. Lipinska, E. Piotrowska, B.J. Oleksyn, Acta Crystallogr. C41 (1985) 977.
[32] M.S. Arias, A. Cosme, E. Gálvez, F. Florencio, I. Fonseca, J. Sanz, Magn. Reson. Chem. 29 (1991) 1130.
[33] A. Meyerhoffer, D. Calstrom, Acta Crystallogr. B25 (1969) 1119.
[34] J.P. Reboul, J.C. Soyfer, B. Cristau, C. Caranoni, G. Pepe, Acta Crystallogr. B38 (1982) 2633.
[35] E. Gálvez-Ruano, I. Iriepa, A. Morreale, D.B. Boyd, J. Mol. Graph. Model. 20 (2001) 183 (and references cited therein).
[36] C. Chang, D.S.C. Yang, C.S. Yoo, B. Wang, J. Pletcher, M. Sax, C.F. Terrence, Acta Crystallogr. B38 (1982) 2065.
[37] V.N. Goka, G. Schlewer, J.M. Linget, J.P. Chambon, C.G. Wermuth, J. Med. Chem. 34 (1991) 2547.
[38] E. Breitmaier, W. Voelter, Carbon-13 NMR Spectroscopy. High-Resolution Methods and Applications in Organic Chemistry and Biochemistry, Verlag, Weinheim, 1987.
[39] F.W. Wehrli, A.P. Marchand, S. Wehrli, Interpretation of Carbon-13 Spectra, second ed., Wiley, Chichester, 1988.